Proc. Natl. Acad. Sci. USA
Vol. 96, pp. 3546–3551, March 1999
Biochemistry

Biochemical characterization of Wnt-Frizzled interactions using a soluble, biologically active vertebrate Wnt protein

JEN-CHIH HSIEH*, AMIR RATTNER*†, PHILIP M. SMALLWOOD*†, AND JEREMY NATHANS*†‡§

*Department of Molecular Biology and Genetics, ‡Departments of Neuroscience and Ophthalmology, and †Howard Hughes Medical Institute, Johns Hopkins University School of Medicine, Baltimore, MD 21205

Contributed by Jeremy Nathans, January 20, 1999

ABSTRACT **Biochemical studies of Wnt signaling have been hampered by difficulties in obtaining large quantities of soluble, biologically active Wnt proteins. In this paper, we report the production in *Drosophila* S2 cells of biologically active *Xenopus* Wnt8 (XWnt8). Epitope- or alkaline phosphatase-tagged XWnt8 proteins are secreted by concentrated S2 cells in a form that is suitable for quantitative biochemical experiments with yields of 5 and 0.5 mg per liter, respectively. Conditions also are described for the production in 293 cells of an IgG fusion of the cysteine-rich domain (CRD) of mouse Frizzled 8 with a yield of 20 mg/liter. We demonstrate the use of these proteins for studying the interactions between soluble XWnt8 and various Frizzled proteins, membrane anchored or secreted CRDs, and a set of insertion mutants in the CRD of *Drosophila* Frizzled 2. In a solid phase binding assay, the affinity of the XWnt8-alkaline phosphatase fusion for the purified mouse Frizzled 8-CRD-IgG fusion is ≈9 nM.**

The Wnt proteins define a large family of extracellular signaling molecules found throughout the animal kingdom. Wnts play a central role in central nervous system, renal, placental, and limb development in vertebrates; early embryonic cell fate decisions and cell migration/polarity in *Caenorhabditis elegans*; and segment polarity and muscle specification in *Drosophila* (reviewed in refs. 1–3). Wnts and the Wnt signaling pathway also have been implicated in mammalian carcinogenesis. Although no alterations in Wnt genes have been identified in human cancers, recent studies have shown that increased activity of the Wnt signaling pathway, mediated by stabilization of β-catenin, is an important aspect of carcinogenesis in human melanomas and colorectal cancers (4–7).

Current evidence indicates that the Frizzled family of integral membrane proteins act as Wnt receptors. The founding member of this family was identified in *Drosophila* based on its role in tissue polarity in the adult cuticle (8). Many additional family members have been identified in both vertebrates and invertebrates, and all have at the amino terminus a conserved extracellular cysteine-rich domain, referred to as the cysteine-rich domain (CRD), that spans ≈120 amino acids and contains 10 invariant cysteines, followed by seven putative membrane spanning domains (9–11). The identification of Frizzled proteins as Wnt receptors arose from experiments in cell culture showing that Frizzled-2, a second Frizzled family member from *Drosophila*, confers wingless (Wg) binding and Wg-dependent stabilization of Armadillo (the *Drosophila* orthologue of β-catenin) (12). Additional evidence for this inference comes from genetic interactions between pairs of Wnt and Frizzled genes in both embryonic and larval development in *C. elegans* (13–15), from RNA injection experiments in *Xenopus* embryos in which a mammalian Frizzled protein was shown to alter the subcellular localization (16) or to change the developmental effects of a coexpressed Wnt (17, 18), and most recently from genetic studies in *Drosophila* that show that Frizzled and Frizzled-2 function redundantly in the embryo as Wg receptors (refs. 19–21; P. Bhanot, R. Nusse, J.N., and K. Cadigan, unpublished work). Tissue culture and *Xenopus* embryo experiments also provide evidence for specificity in Wnt and Frizzled interactions: some, but not all, Frizzled proteins confer Wg binding in transfected cells (12), and axis induction by *Xenopus* Wnt5A (XWnt5A) is conferred by only one of seven Frizzled proteins examined (17).

An additional level of complexity in Wnt signaling has emerged with the discovery in vertebrates of a family of secreted proteins that possess a CRD resembling those present in the Frizzled proteins; the members of this family are referred to as secreted Frizzled related proteins (sFRP) (22–28). Among Frizzled proteins, the CRD contains some or all of the Wnt-binding determinants because it is both necessary and sufficient for conferring Wg binding to transfected cells (12). sFRPs also can bind to Wnts, presumably via the CRD, when either protein is artificially anchored to the plasma membrane (23, 26). In *Xenopus* embryos, one sFRP, sFRP-3/FRZB, is localized to Spemann's organizer, and injection of RNA encoding any of several sFRPs inhibits the bioactivity of coinjected XWnt8 (22–24, 27, 28). These and other data suggest that the sFRPs normally act as competitive inhibitors of Wnt-Frizzled binding.

Despite the advances noted above, the biochemical and structural properties of Wnts and their interactions with Frizzled and sFRP proteins and with extracellular matrix molecules remain poorly defined. The principal challenge is to prepare the requisite quantities of biologically active Wnts in soluble form. Wnts exhibit a low efficiency of secretion and a propensity to adhere to the extracellular matrix (ECM) (29–32), and, as a result, soluble Wnts thus far have only been produced in small quantities and in impure form. For example, biologically active Wg has been produced in the conditioned medium of transfected *Drosophila* Schneider (S2) cells (33), and biologically active Wnt-1 (34) and Wnt-5A (35) have been produced in the conditioned medium of transfected mammalian cells, but none of these preparations have been used for quantitative binding or structural studies.

In this paper, we report the production in *Drosophila* S2 cells of biologically active XWnt8. Epitope- or alkaline phosphatase-tagged XWnt8 proteins are secreted in a form that is suitable for quantitative biochemical experiments. Conditions also are described for the production of an IgG fusion of the CRD of mouse Frizzled 8 (mfz8) in milligram quantities. We demonstrate the use of these proteins for studying the interactions between soluble XWnt8 and various Frizzled proteins, membrane-anchored and

Abbreviations: AP, human placental alkaline phosphatase; CRD, cysteine-rich domain; ECM, extracellular matrix; fz, Frizzled; GPI, glycophosphatidylinositol; PI-PLC, phosphoinositide–phospholipase C; sFRP, secreted Frizzled-related protein; Wg, Wingless; X-phos, 5-bromo-4-chloro-3-indolyl-phosphate; NBT, nitroblue tetrazolium; h, human, m, mouse, D, *Drosophila*; X, *Xenopus*.

§To whom reprint requests should be addressed at: 805 PCTB, 725 North Wolfe Street, Johns Hopkins University School of Medicine, Baltimore, MD 21205. e-mail: jnathans@jhmi.edu.

The publication costs of this article were defrayed in part by page charge payment. This article must therefore be hereby marked "*advertisement*" in accordance with 18 U.S.C. §1734 solely to indicate this fact.

PNAS is available online at www.pnas.org.

secreted CRDs, and a set of insertion mutants in the CRD of *Drosophila* Frizzled 2.

MATERIALS AND METHODS

DNA Constructs. The XWnt8-myc protein contains a carboxyl-terminal myc epitope tag (EQKLISEEDL) inserted between amino acids 339 and 340 (36). The XWnt8—human placental alkaline phosphatase (AP) construct contains the coding region of XWnt8-myc, without the carboxyl-terminal 19 amino acids, fused upstream of the AP catalytic domain in a modified version of pAPtag2, a vector from which the alkaline phosphatase signal sequence has been removed (37). Glycophosphatidylinositol (GPI)-anchored and myc-tagged CRDs were constructed as described in ref. 26 by using a modified pCIS vector (38) in which a DNA segment encoding a myc epitope (39) flanked by glycine spacers (GGGMEQKLISEEDLNGGG) is followed by a segment encoding the carboxyl-terminal 40 amino acids of decay-activating factor (40). To construct the CRD-myc-GPI expression plasmids, PCR products engineered to contain an optimal Kozak sequence around the initiator ATG and encompassing the indicated codons were inserted in-frame and upstream of the myc-GPI cassette: *Drosophila* fz2 (Dfz2), 1–270 (12); mfz3, 1–157; mfz4, 1–181; human fz5 (hfz5), 1–172; mfz6, 1–153; mfz7, 1–185; mfz8, 1–173 (11). Insertion of three codons (5′GGTTCCGGA encoding gly-ser-gly and containing a unique *Bsp*EI site) into each of 23 locations in the Dfz2 CRD was accomplished by PCR amplification with pairs of mutagenic and flanking primers followed by replacement of the wild-type DNA segment with the amplified DNA segment between the *Bam*HI site at codon 58 and either the *Bst*EII site at codon 171 or the *Pst*I site at codon 270. The mfz8CRD-IgG fusion was generated by fusing codons 1–173 of mfz8 upstream of the hinge region of the human IgG heavy chain gene (41). All DNA segments generated by PCR were sequenced to rule out spurious mutations.

Production of XWnt8-myc and XWnt8-AP in S2 Cells. Conditioned medium containing XWnt8-myc or XWnt8-AP was produced in S2 cells stably transfected with the corresponding cDNA under the control of a metallothionein promoter. For protein production, cells were concentrated 4-fold and were incubated at 25°C for 24 hr in serum-free *Drosophila* Expression System medium (Invitrogen) containing 0.5 mM $CuSO_4$. Control medium was produced by $CuSO_4$ induction of untransfected S2 cells. The media were centrifuged at 100,000 × *g* at 4°C for 1 hr to remove aggregates and were concentrated 20-fold by ultrafiltration.

Production of mfz8CRD-IgG Fusion Protein. Mfz8CRD-IgG and IgG were produced in 293 cells that were transiently transfected by using Lipofectamine (GIBCO/BRL). One day after transfection, cells were transferred to serum-free DMEM/F-12, and the secreted protein was harvested after an additional 24 hr. Control conditioned medium was obtained from untransfected 293 cells. For some experiments, mfz8CRD-IgG and IgG were affinity purified by using protein A Sepharose (Amersham Pharmacia) with a low pH elution. Protein concentrations were estimated by visual comparison with a BSA standard after SDS/PAGE and Coomassie blue staining.

β-Catenin Stabilization Assay. C57MG cells were grown in 35-mm wells in DMEM supplemented with 10% fetal bovine serum and 10 μg/ml insulin and were ≈70% confluent at the time of the assay. Cells were washed once with serum-free DMEM/F-12 and were incubated at the indicated temperature with 0.8 ml of S2-conditioned medium that was diluted with an equal volume of serum-free DMEM/F-12. Heparin (molecular weight = 6,000; Sigma) was added as indicated. After a 3-hr incubation, the conditioned medium was removed, and cells were harvested by incubation at 4°C for 5 min in PBS containing 5 mM EDTA and were collected by centrifugation. The cells were resuspended and homogenized in 100-μl lysis buffer (10 mM Tris·HCl, pH 7.5/140 mM NaCl/5 mM EDTA/0.5 μg/ml leupeptin/0.5 μg/ml aprotinin/0.5 μg/ml antipain), followed by centrifugation at 800 × *g* for 2 min. The resulting supernatant was further centrifuged at 100,000 × *g* for 30 min at 4°C, and the proteins in the high speed supernatant (containing cytoplasmic β-catenin) were separated in a SDS/7.5% polyacrylamide gel and were immunoblotted by using anti-β-catenin mAb 15B8 (Sigma).

Phosphoinositide–Phospholipid C (PI-PLC) Release of GPI-Anchored Proteins. COS cells in 35-mm wells were transfected with 2 μg of plasmid DNA and 4 μl of FuGene 6 transfection reagent (Boehringer Mannheim). Twenty-four hours after transfection, the cells were harvested, were centrifuged at 800 × *g* for 2 min, and were resuspended in 100 μl of PBS containing 5 mM EDTA and 10 units of PI-PLC (Boehringer Mannheim). After a 1-hr incubation at 37°C with gentle rotation, the supernatant containing the released proteins was separated from the cells by centrifugation at 800 × *g* for 2 min. The cell pellet was resuspended in 100 μl of solublization buffer (20 mM Hepes, pH 7.2/150 mM NaCl/1 mM EGTA/1 mM EDTA/10% glycerol/1% Triton X-100), was incubated on ice for 10 min, and was centrifuged at 4°C for 2 min at 800 × *g* to remove nuclei and cell debris.

Binding of XWnt8-AP and Antibodies to Transfected Cells. For staining under nonpermeablized condition, live transfected COS cells growing on coverslips were incubated at room temperature for 1 hr with anti-myc mAb 9E10 (39) diluted 1:1,000 in culture medium or with XWnt8-AP-conditioned medium diluted with an equal volume of DMEM/F-12. After binding, cells either were washed three times with DMEM/F12 and were fixed in 2% methanol-free formaldehyde/PBS or were washed three times with binding buffer (0.5 mg/ml BSA in Hank's balanced salt solution with 20 mM Hepes, pH 7.0), were fixed for 30 sec in 60% acetone, 3% formaldehyde in 20 mM Hepes (pH 7.0), and were washed twice with binding buffer. For anti-myc staining, the fixed cells were incubated at room temperature with Texas Red-conjugated anti-mouse antibody (Vector Laboratories) diluted 1:200 in 5% goat serum in PBS, followed by three washes in PBS. For XWnt8-AP staining, the fixed cells in 20 mM Hepes (pH 7.0), 150 mM NaCl were incubated at 65°C for 100 min, were washed once in AP buffer (0.1 M Tris·HCl, pH 9.4/0.1 M NaCl/5 mM NaCl) and were stained at room temperature overnight with 5-bromo-4-chloro-3-indolyl-phosphate (X-phos) (165 μg/ml)/nitroblue tetrazolium (NBT) (330 μg/ml) in AP buffer. For anti-myc staining under permeabilized condition, the transfected cells were fixed in 60% acetone, 3% formaldehyde in 20 mM Hepes (pH 7.0) before antibody incubation.

Solution Binding Assay. Twelve micrograms of IgG or mfz8CRD-IgG were prebound to protein A Sepharose beads and were incubated for 16 hr at 4°C with 500 μl of 4-fold-concentrated XWnt8-myc-conditioned medium. The beads were separated by centrifugation into bound and unbound fractions and then were washed over 10 minutes at 4°C with three changes of Hank's balanced salt solution with 20 mM Hepes (pH 7.0).

Solid Phase Binding Assay. One-hundred microliters of 293 cell conditioned medium containing 2 μg of Mfz8CRD-IgG or IgG alone was used to coat each well of a 96-well tray at 4°C overnight. The unoccupied sites in the wells were blocked at 4°C for 4 hr with 200 μl of 2 mg/ml BSA in wash buffer [Hank's balanced salt solution with 20 mM Hepes (pH 7.0)]. After three washes in wash buffer, XWnt-AP-conditioned medium diluted in 2 mg/ml BSA in wash buffer was added to the coated wells. After incubation at 4°C for 20 hr, the wells were washed five times with 200 μl of wash buffer. Two-hundred microliters of 150 mM p-nitrophenyl phosphate in 1 M diethanolamine (pH 9.8), 1 mM $MgCl_2$ was added to each well, and the change in absorbance at 405 nm was measured.

RESULTS

Production of XWnt8-myc and XWnt8-AP in S2 Cells. Our attempts to produce a soluble vertebrate Wnt protein for biochemical experiments have focused on XWnt8 because Moon and colleagues (36, 42) have observed that addition of a myc

epitope tag near the XWnt8 carboxyl terminus, a construct referred to here as XWnt8-myc, is compatible with biological activity in *Xenopus* embryos. As an expression system, we have chosen *Drosophila* Schneider (S2) cells, which, as noted above, have been used successfully to produce bioactive Wg (33) as well as a variety of other secreted vertebrate proteins (43). Fig. 1*A* shows that S2 cells can secrete both XWnt8-myc and a fusion of XWnt8-myc and the catalytic domain of human placental alkaline phosphatase (XWnt8-AP). A comparison of the anti-myc immunoblot signals from XWnt8-myc and XWnt8-AP and from a myc-tagged derivative of the *Escherichia coli* maltose binding protein indicates that XWnt8-myc and XWnt8-AP are secreted from concentrated S2 cells with yields up to ≈5 and ≈0.5 mg/liter, respectively.

The biological activity of XWnt8-myc was tested by applying S2-conditioned medium containing XWnt8-myc or control S2 conditioned medium to C57MG cells and monitoring the stabilization of cytoplasmic β-catenin (Fig. 1*B*; ref. 44). In these experiments, we observed significant β-catenin stabilization if the incubation was performed at 23°C but little or no stabilization at 37°C. XWnt8-myc activity was enhanced by the inclusion of heparin, with a maximal effect at 0.1–0.5 μg/ml. The temperature sensitivity of XWnt8-myc activity on C57MG cells could reflect either instability of XWnt-8-myc and/or associated proteins from S2 cells or a temperature-dependence of β-catenin turnover in C57MG cells. XWnt8-myc is also active in stabilizing Armadillo in *Drosophila* clone 8 cells, an imaginal disc cell line, but the degree of stabilization is severalfold lower than that obtained with similarly prepared S2 conditioned medium containing Wg (data not shown). XWnt8-myc produced in transiently transfected 293 cells was secreted with an efficiency ≈10-fold lower than that observed for S2 cells (Fig. 1*A*) and was inactive in the β-catenin stabilization assay and in Frizzled binding assays (data not shown).

Cell Surface Binding of XWnt8-AP to Frizzled Proteins and Frizzled CRDs. The XWnt8-AP fusion protein described above provides a convenient and quantitative probe to investigate the binding of Wnt and Frizzled proteins. When conditioned medium containing XWnt8-AP was incubated at room temperature with live COS or 293 cells and subsequently was visualized with a X-phos/NBT tetrazolium histochemical reaction, little or no cell-associated AP activity was observed, indicating that this fusion protein does not bind significantly to either plasma membrane proteins or the ECM produced by these two cell lines. This behavior is in contrast to that of Wg produced by S2 cells, which adheres to the ECM of a variety of cultured cells. Specific binding of Wg to cell surface Frizzled proteins only has been observed after heparitinase pretreatment to decrease ECM binding (12). Transient transfection of COS or 293 cells with Dfz2, mfz4, hfz5, mfz7, mfz8, and Xfz8 conferred cell surface XWnt8-AP binding whereas transfection with mfz3 and mfz6 did not, a pattern identical to that observed previously for Wg (Table 1 and Fig. 2*B*; ref. 12). Binding experiments with control conditioned medium from untransfected S2 cells shows no alkaline phosphatase staining of COS cells transfected with Dfz2, mfz4, or hfz5, indicating that the observed Frizzled binding activity derives from XWnt8-AP. In these experiments, absence of XWnt8-AP binding could reflect a low affinity between ligand and receptor or a defect in the stability, folding, or surface localization of the Frizzled protein. Therefore, to measure the surface localization of each receptor protein in a uniform manner and also to assess the binding of XWnt8-AP to the various Frizzled CRDs in the absence of the Frizzled membrane spanning domains, we constructed a set of myc-tagged and GPI-anchored derivatives of each CRD (Fig. 2).

Incubation of XWnt8-AP with transfected cells expressing CRD-myc-GPI constructs from Dfz2, mfz3, mfz4, hfz5, mfz6, mfz7, and mfz8 reveals the same relative efficiency of XWnt8-AP

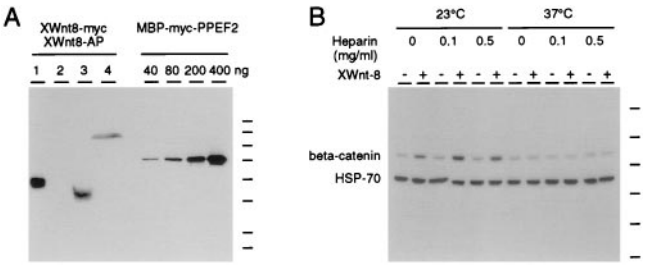

FIG. 1. Secretion of biologically active XWnt8-myc by S2 cells. (*A*) Immunoblot using anti-myc mAb. (*Left*) Lanes: 1, 32 μl of 40-fold concentrated conditioned medium from 293 cells transfected with XWnt8-myc; 2, 32 μl of 4-fold concentrated conditioned medium from untransfected S2 cells; 3, 32 μl of 4-fold concentrated conditioned medium from S2 cells transfected with XWnt8-myc; 4, 32 μl of 80-fold concentrated conditioned medium from S2 cells transfected with XWnt8-myc-AP. (*Right*) Dilution series of a purified fusion protein used as an immunoblot standard; the fusion protein contains the myc epitope flanked by the *E. coli* maltose binding protein at the amino terminus and an ≈15-kDa segment of a ser/thr protein phosphatase at the carboxyl terminus (57), a configuration that eliminates problems in quantitation that might arise from proteolytic cleavage of an epitope fused to either of the two termini. Molecular mass standards are 194, 120, 87, 64, 52, 39, 26, and 21 kDa. (*B*) XWnt8-myc stabilizes β-catenin in C57MG cells at room temperature, and this activity is enhanced by heparin. Conditioned medium from untransfected S2 cells (−) or XWnt8-myc transfected S2 cells (+) in the presence of the indicated concentration of heparin was applied to C57MG cells at either 23 or 37°C as indicated. Cytosolic proteins were prepared, and β-catenin was visualized with mAb 15B8. To control for equal loading, HSP-70 was visualized with mAb BRM-22 (Sigma). Molecular mass standards are 194, 120, 87, 64, 52, and 39 kDa.

Table 1. Semiquantitative assessment of XWnt8-AP binding to different Frizzled and CRD-myc-GPI proteins based on X-phos/NBT staining of live, transiently transfected COS cells

Frizzled	Full-length protein	CRD-myc-GPI
mfz3	−	−
mfz4	++	++
hfz5	++	++
mfz6	−	−
mfz7	+	+
mfz8	++	++
Xfz8	++	ND
Dfz2	++	++
1. Dfz2 (66GSG67)	−	−
2. Dfz2 (68GSG69)	−	−
3. Dfz2 (73GSG74)	−	−
4. Dfz2 (80GSG81)	−	−
5. Dfz2 (85GSG86)	++	+
6. Dfz2 (89GSG90)	−	−
7. Dfz2 (92GSG93)	−	−
8. Dfz2 (96GSG97)	−	−
9. Dfz2 (102GSG103)	++	++
10. Dfz2 (106GSG107)	++	++
11. Dfz2 (111GSG112)	+	−
12. Dfz2 (114GSG115)	−	−
13. Dfz2 (126GSG127)	+	+
14. Dfz2 (128GSG129)	++	++
15. Dfz2 (130GSG131)	+	−
16. Dfz2 (137GSG138)	−	−
17. Dfz2 (141GSG142)	−	−
18. Dfz2 (144GSG145)	++	−
19. Dfz2 (152GSG153)	++	++
20. Dfz2 (160GSG161)	++	+
21. Dfz2 (165GSG166)	−	−
22. Dfz2 (172GSG173)	++	+
23. Dfz2 (174GSG175)	++	++

The three amino acid insertion mutants are referred to by the codon numbers flanking the gly-ser-gly insertion. For example, 66GSG67 refers to the insertion of the nine nucleotides encoding gly-ser-gly between codons 66 and 67. ++, strong binding; +, weak binding; −, undetectable binding. ND, not determined.

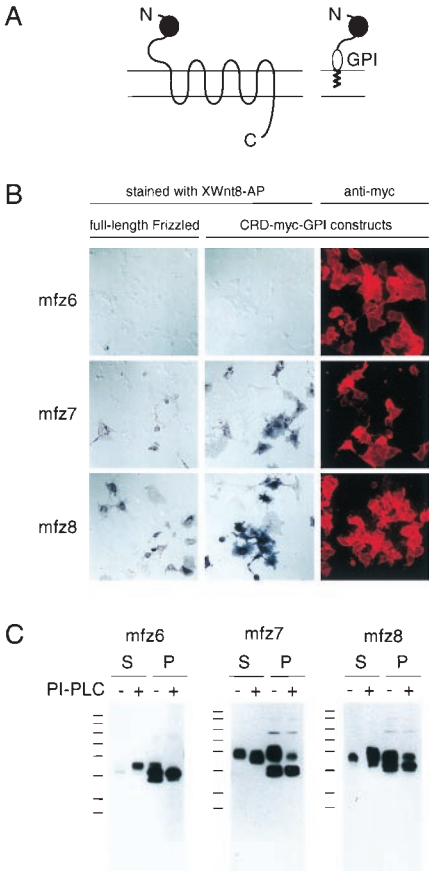

FIG. 2. Binding of XWnt8-AP to full-length Frizzled proteins and the corresponding GPI-anchored CRDs on the surface of transfected COS cells. (*A*) Schematic diagram showing the location of the CRD (filled ball) in a full-length Frizzled protein and in a CRD-myc-GPI construct. Horizontal lines represent the membrane, and zigzag lines represent the lipid component of GPI. N, amino terminus; C, carboxyl terminus. (*B* and *C*) XWnt8-AP binding and surface localization assays for three Frizzled proteins that show undetectable binding (mfz6), intermediate binding (mf7), and strong binding (mfz8). (*B*) Light microscopy of representative samples of COS cells transiently transfected with the indicated full-length Frizzled (left column) or the corresponding Frizzled CRD-myc-GPI construct (center and right columns). Live cells were stained with XWnt8-AP (left and center columns) or with anti-myc mAb and a fluorescent secondary antibody (right column). The cells remained intact during the binding reaction as determined by the failure of the anti-myc mAb to bind myc-tagged Dishevelled (a cytoplasmic protein) under these conditions; fixation and permeabilization with acetone and paraformaldehyde before incubation with the anti-myc mAb led to intense staining of myc-tagged Dishevelled (data not shown). (*C*) PI-PLC release of GPI-anchored CRDs from the surface of live cells. Transfected COS cells were incubated in the absence (−) or presence (+) of PI-PLC, and, after centrifugation, the released protein was recovered from the supernatant (S) and the cells were recovered from the pellet (P). Proteins were resolved by SDS/PAGE and were visualized with anti-myc mAb immunoblotting. Molecular mass standards are 194, 120, 87, 64, 52, 39, 26, and 21 kDa.

binding as seen with the corresponding full-length Frizzled proteins. When live cells transfected with each CRD-myc-GPI construct were immunostained with anti-myc mAbs, similar levels of cell-surface CRD-myc-GPI protein were observed in each case (Fig. 2*B* and data not shown). As an independent measure of plasma membrane localization of the CRD-myc-GPI proteins, live cells expressing each of the seven constructs were treated with PI-PLC to cleave the GPI anchor and release the surface-accessible protein into the medium. Anti-myc immunoblotting of the CRD-myc-GPI proteins showed that, in each case, three major electrophoretic species are observed, presumably reflecting different patterns of glycosylation. The protein released by PI-PLC treatment corresponds to the lowest mobility species, suggesting that this species is the only one present at the cell surface. The cell surface CRD-myc proteins were released by PI-PLC treatment with yields that range from 10 to 30% of the total CRD-myc-GPI protein, suggesting that in each case a significant fraction of the CRD protein is able to fold correctly and move through the endoplasmic reticulum–Golgi-plasma membrane pathway (Fig. 2*C* and data not shown; ref. 45). Because each of the different CRD-myc-GPI proteins is available for binding, these experiments demonstrate that XWnt8-AP binds efficiently to the CRDs of Dfz2, mfz4, hfz5, mfz7, and mfz8 but binds poorly or not at all to the CRDs of mfz3 and mfz6.

XWnt8-AP Binding to Insertion Mutants of Dfz2. To begin to define the regions of the CRD that mediate Wnt binding, we measured the binding of XWnt8-AP to live cells that had been transfected with a series of 23 insertion mutants in the CRD of Dfz2 (Fig. 3*A*). Insertional mutagenesis was performed with a three-codon cassette that codes for gly-ser-gly, an insertion that would be predicted to sterically disrupt binding if located at any point on the ligand-binding surface. Failure to bind XWnt8-AP also could reflect a defect in the folding or stability of the CRD. To minimize the probability that the tripeptide insertion might cause a structural defect, the 23 insertions were placed at least one amino acid from any cysteine and within those regions that are most hydrophilic. Given the predicted flexibility of the gly-ser-gly tripeptide (46), we presume that most insertions within surface loops would be compatible with a correctly folded CRD.

Each of the 23 insertion mutants was studied in the context of the full-length Dfz2 protein and in a CRD-myc-GPI construct. After transfection, the efficiency of plasma membrane localization was determined for each CRD-myc-GPI mutant by immunostaining of live cells with anti-myc mAbs and by PI-PLC digestion of live cells followed by immunoblotting as described above (Fig. 3 *B* and *C*). Of interest, all 23 mutants resemble wild-type Dfz2-CRD-GPI in showing robust cell surface immunostaining and significant release of the low mobility electrophoretic species on PI-PLC treatment (corresponding to 10–30% of the total Dfz2-CRD protein), indicative of a high degree of plasma membrane localization. On the assumption that passage through the endoplasmic reticulum–Golgi-plasma membrane pathway reflects correct folding (45), this result implies that the native CRD structure can tolerate insertions at each of these positions. This observation raises the possibility that the CRD may be a relatively extended structure with a high surface to volume ratio.

Different Dfz2 insertion mutants differ markedly in XWnt8-AP binding when assayed on the surface of live transfected cells (Table 1 and Fig. 3*B*). Mutants 15 and 18 (130GSG131 and 144GSG145) bind XWnt8-AP when they are present in the context of the full-length Dfz2 sequence but fail to bind as GPI-anchored CRDs, suggesting the possibility that stabilizing interactions may occur between the membrane-embedded domain of the Frizzled protein and the CRD or the CRD-Wnt complex. Among the Dfz2CRD-GPI mutants, 5 bind with a strength indistinguishable from that of the wild type, 4 bind weakly, and 14 fail to bind. Binding and nonbinding mutants are distributed throughout the length of the CRD with nonbinding mutants showing significant clustering.

Quantitative Binding of XWnt8-AP to mfz8CRD-IgG. The binding of soluble XWnt8-AP to membrane-anchored CRDs suggests that these proteins also might interact if the CRD is produced as a secreted molecule. To test this idea, we produced the mfz8 CRD as an amino-terminal fusion with a human IgG heavy chain (mfz8CRD-IgG) in transfected 293 cells. In this expression system, mfz8CRD-IgG accumulates to ≈20 mg/liter and can be purified to apparent homogeneity with protein A Sepharose (Fig. 4*A*).

In an initial experiment, we determined the efficiency of coprecipitation of XWnt8-myc with mfz8CRD-IgG or with the IgG backbone alone (Fig. 4*B*). This experiment indicates that at least 90% of the secreted XWnt8-myc is competent to specifically

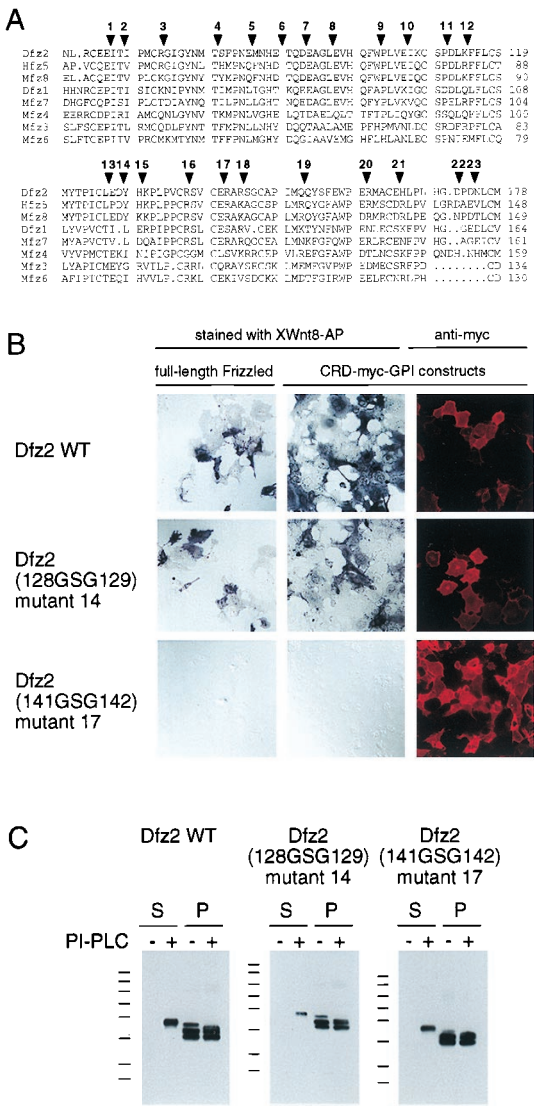

FIG. 3. Binding of XWnt8-AP to tripeptide insertion mutants within the Dfz2 CRD. For the wild type and for each mutant, the experiments were performed with both full-length Dfz2 and the corresponding GPI-anchored CRDs displayed on the surface of transfected COS cells. (*A*) Alignment of CRDs from a subset of Frizzled proteins showing the locations of the 23 gly-ser-gly insertion mutations. (*B*) Light microscopy of representative samples of COS cells transiently transfected with the indicated full-length Dfz2 (left column) or the corresponding Dfz2 CRD-myc-GPI construct (center and right columns). Examples are shown for wild-type Dfz2, Dfz2 mutant 14 (128GSG129), which shows strong binding and Dfz2 mutant 17 (141GSG142), which shows no detectable binding. Live cells were stained with XWnt8-AP (left and center columns) or with anti-myc mAb and a fluorescent secondary antibody (right column), as described for Fig. 2. (*C*) PI-PLC release of GPI-anchored Dfz2 CRDs from the surface of live cells, as described for Fig. 2. Molecular mass standards are 194, 120, 87, 64, 52, 39, 26, and 21 kDa.

bind mfz8CRD-IgG. These reagents then were used to develop a solid phase enzyme-linked binding assay in which varying concentrations of soluble XWnt8-AP were incubated with immobilized mfz8CRD-IgG or IgG in the wells of a 96-well tray (Fig. 4*C*). Four independent experiments using either crude conditioned medium containing mfz8CRD-IgG, which is ≈80% pure, or Protein A Sepharose purified mfz8CRD-IgG yielded similar results. When redrawn as a Scatchard plot and fit to a single line, the binding data indicate an average affinity of 9 ± 2 nM (n = 4). However, close examination of the Scatchard plots suggests that two or more classes of sites may better represent the binding

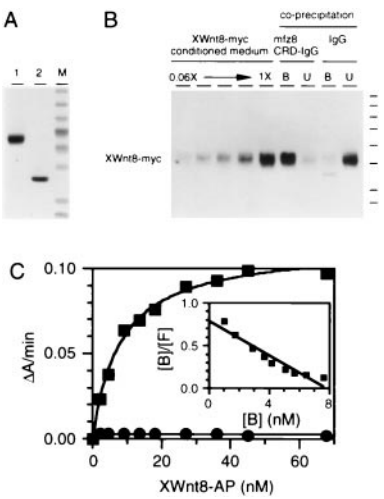

FIG. 4. Binding of XWnt8-myc and XWnt8-AP to mfz8CRD-IgG. (*A*) Coomassie-stained gel with mfz8CRD-IgG (lane 1) or the IgG fusion partner alone (consisting of the hinge and F_c regions) (lane 2) secreted from transfected 293 cells and purified by using protein A Sepharose. Molecular mass standards are 194, 120, 87, 64, 52, 39, 26, 21, and 15 kDa. (*B*) Binding efficiency of XWnt8-myc with IgG or mfz8CRD-IgG prebound to protein A Sepharose beads. Equal fractions of the bound (B), unbound (U), or starting material (1X) were analyzed by SDS/PAGE and anti-myc immunoblotting. A 2-fold dilution series of the starting material is shown at left. Greater than 90% of XWnt8-myc was bound to mfz8CRD-IgG, with little or no binding to IgG. Molecular mass standards are 194, 120, 87, 64, 52, 39, 26, and 21 kDa. (*C*) Solid phase binding of XWnt8-AP to IgG (circles) or mfz8CRD-IgG (squares). The rate of hydrolysis of p-nitrophenyl phosphate (measured as the rate of change in absorbance at 405 nm) is plotted against XWnt8-myc concentration. *Inset* shows a Scatchard plot of the binding data fit to a single straight line, which yields a calculated K_d of 8 nM. B, bound; F, free.

data; under an assumption of two sites, the estimated affinities of the two sites would be predicted to differ by ≈10-fold.

DISCUSSION

Production of Soluble Wnt and Frizzled Derivatives. Producing soluble, biochemically well behaved Wnts has been a longstanding goal in this field but has been problematic. Producing secreted Frizzled or sFRP CRDs, the domain implicated in Wnt binding, either alone or as fusion proteins with IgG or AP, also has proven difficult because most are poorly secreted (A.R., J.-C.H., and J.N., unpublished data). The several examples described in the present report represent that minority of constructs and host–vector systems for which we have observed good yields of apparently native proteins. In the case of XWnt8, this could reflect the presence in S2 cells of putative chaperones such as the porcupine protein (47, 48), as yet uncharacterized proteins in the conditioned medium that might associate with XWnt8, or the low temperature (23°C) at which S2 cells are grown. The efficient secretion of mfz8CRD-IgG from transfected 293 cells—≈20 mg/liter—may reflect a serendipitous choice of the fusion point between the CRD and the IgG heavy chain in this construct.

Structural and Functional Mapping of the CRD. The analysis of 23 tripeptide insertion mutants in the Dfz2 CRD identifies a set of discontinuous segments along the linear sequence where insertion results in loss of XWnt8-AP binding. These are presumed to be sites of direct or close contact with the XWnt8-AP ligand. Other regions where tripeptide insertion fails to diminish XWnt8-AP binding can be eliminated as sites of close contact. The loss of XWnt8-AP binding caused by several tripepeptide insertions in the carboxyl-terminal two-thirds of the CRD is at odds with the results of Lin *et al.* (49) in which coimmunoprecipitation was observed between cotransfected Wnt-1 and various sFRP-3 derivatives, including deletion derivatives lacking large parts of the CRD. This discrepancy may be related to the

significant endoplasmic reticulum retention that is characteristic of both Wnts and sFRPs, which suggests that much of the association observed between these proteins in cotransfected cells represents aggregation of misfolded proteins. These conflicting data serve to emphasize the importance for binding experiments of starting with biochemically well behaved proteins.

Specificity of Wnt-CRD Binding. The available data for Wnt-Frizzled and Wnt-sFRP binding at the surface of transfected cells (refs. 12, 23, and 26 and this report) indicates that some Wnts can bind to multiple Frizzled and/or sFRP targets. For example, a *Drosophila* Wnt, Wg, binds with similar efficiency to a subset of mammalian Frizzled proteins and to *Drosophila* Frizzled and Frizzled-2 (12). Here, we show that a *Xenopus* Wnt, XWnt8, binds with similar efficiency to *Drosophila* fz2 and the same set of mammalian Frizzled proteins to which Wg binds.

One explanation for this apparent promiscuity in binding is that semiquantitative cell surface binding assays do not reveal small but biologically significant differences in affinity. This possibility can be investigated by extending the quantitative enzyme-linked binding assay described here to cell-surface measurements and by determining the binding affinities of additional pairs of Wnts and CRD-IgG fusions. It is also possible that additional factors associate with Wnts, Frizzled proteins, or sFRPs *in vivo* to modify and/or narrow the specificity of their interactions. These factors might include heparin, other ECM components, coreceptors, plasma membrane lipids, and additional secreted proteins. The plausibility of these more complex interactions is supported by the well known affinity of Wnts for heparin and other ECM components (e.g., ref. 31), the ability of heparin and other ECM components to modulate Wnt signaling *in vitro* (ref. 50 and this report), the affinity of the carboxyl-terminal domain of at least two of the sFRPs for heparin (ref. 22; A.R., J.-C.H., and J.N., unpublished work), and the recent discovery of Wnt inhibitory factor-1, a secreted Wnt-binding protein that lacks a CRD (51). *In vivo* evidence for the importance of the ECM in Wnt signaling comes from the effects of mutations in proteoglycan biosynthetic genes in *Drosophila* (52–54).

Despite the evidence for additional cofactors, the *in vitro* binding experiments with mfz8CRD-IgG show that affinities of <10 nM are obtained with the CRD alone. These experiments imply that the Frizzled transmembrane domains, plasma membrane lipids, ECM, and putative coreceptors do not play an obligatory role in Wnt-Frizzled binding. In particular, the solid phase binding assay shows that heparin does not alter the affinity of XWnt8-AP for mfz8CRD-IgG, although it enhances β-catenin stabilization induced by XWnt8-myc treatment of C57MG cells. These data suggest that the role of heparin in Wnt signal transduction may not involve a direct effect on receptor–ligand binding, a possibility that would be in contrast to the direct role of heparin in fibroblast growth factor dimerization and receptor binding (55, 56). We note that the experiments reported here do not rule out the possibility that other proteins in the S2 conditioned medium may associate with XWnt8 and participate in the binding reaction.

Wnt, Frizzled, and sFRP proteins are all members of large families. To date, 15 Wnt, 9 Frizzled, and 5 sFRP genes have been identified in mammals, and several Wnt and Frizzled genes have been identified in *Drosophila* and in *C. elegans*. The broad and overlapping patterns of expression seen for many of these genes raises the possibility of multiple Wnt-Frizzled and Wnt-sFRP interactions. There is currently little quantitative information regarding the affinity and specificity of interactions among individual members of these protein families *in vitro*, and, in most cases, it is not yet known which family members interact in a biologically meaningful manner *in vivo*. The *in vitro* interactions observed among several Wnt, Frizzled, and sFRP proteins from diverse vertebrate and invertebrate species indicate that the relevant protein–protein interfaces have been conserved during evolution and suggests that many pairs of family members may have the potential to interact.

The authors thank Dr. Randy Moon for the XWnt8-myc plasmid; Dr. Peter Klein for Xfz8; Dr. Brian Seed for the human IgG cDNA; Dr. John Flanagan for the AP cDNA; Dr. Ingrid Caras for the decay activating factor cDNA; and Drs. Phil Beachy and Dan Leahy for comments on the manuscript. This work was supported by the Howard Hughes Medical Institute.

1. Cadigan, K. M. & Nusse, R. (1997) *Genes Dev.* **11,** 3286–3305.
2. Moon, R. T., Brown, J. D. & Torres, M. (1997) *Trends Genet.* **13,** 157–162 (1997).
3. Nusse, R. & Varmus, H. (1992) *Cell* **69,** 1073–1087.
4. Munemitsu, S., Albert, I., Souza, B., Rubinfeld, B. & Polakis, P. (1995) *Proc. Natl. Acad. Sci. USA* **92,** 3046–3050.
5. Korinek, V., Barker, N., Morin, P. J., van Wichen, D., deWeger, R., Kinzler, K. W., Vogelstein, B. & Clevers, H. (1997) *Science* **275,** 1784–1787.
6. Morin, P. J., Sparks, A. B., Korinek, V., Barker, N., Clevers, H., Vogelstein, B. & Kinzler, K. W. (1997) *Science* **275,** 1787–1790.
7. Rubinfeld, B., Robbins, P., El Gamil, M., Albert, I., Porfiri, E. & Polakis, P. (1997) *Science* **275,** 1790–1792.
8. Adler, P. N. (1992) *BioEssays* **14,** 735–741.
9. Vinson, C., Conover, S. & Adler, P. N. (1989) *Nature (London)* **338,** 263–264.
10. Chan, S. D. H., Karpf, D. B., Fowlkes, M. E., Hooks, M., Bradley, M. S., Vuong, V., Bambino, T., Liu, M. Y. C., Arnaud, C. D., Strewler, G. J., *et al.* (1992) *J. Biol. Chem.* **267,** 25202–25207.
11. Wang, Y., Macke, J. P., Abella, B. S., Andreasson, K., Worley, P., Gilbert, D. J., Copeland, N. G., Jenkins, N. A. & Nathans, J. (1996) *J. Biol. Chem.* **271,** 4468–4476.
12. Bhanot, P., Brink, M., Harryman Samos, C., Hsieh, J.-C., Wang, Y., Macke, J. P., Andrew, D., Nathans, J. & Nusse, R. (1996) *Nature (London)* **382,** 225–230.
13. Sawa, H., Lobel, L. & Horvitz, H. R. (1996) *Genes Dev.* **10,** 2189–2197.
14. Rocheleau, C. E., Downs, W. D., Lin, R., Wittmann, C., Bei, Y., Cha, Y.-H., Ali, M., Priess, J. R. & Mello, C. C. (1997) *Cell* **90,** 707–719.
15. Thorpe, C. J., Schlesinger, A., Carter, J. C. & Bowerman, B. (1997) *Cell* **90,** 695–705.
16. Yang-Snyder, J., Miller, J. R., Brown, J. D., Lai, C.-J. & Moon, R. T. (1996) *Curr. Biol.* **6,** 1302–1306.
17. He, X., Saint-Jeannet, J.-P., Wang, Y., Nathans, J., Dawid, I. & Varmus, H. (1997) *Science* **275,** 1652–1654.
18. Deardorff, M. A., Tan, C., Conrad, L. J. & Klein, P. S. (1998) *Development (Cambridge, U.K.)* **125,** 2687–2700.
19. Kennerdell, J. R. & Carthew, R. W. (1998) *Cell* **95,** 1017–1026.
20. Bhat, K. M. (1998) *Cell* **95,** 1027–1036.
21. Muller, H.-A. J., Samanta, R. & Wieschaus, E. (1999) *Development (Cambridge, U.K.)* **126,** 577–586.
22. Finch, P. W., He, X., Kelley, M. J., Uren, A., Schaudies, R. P., Popescu, N. C., Rudikoff, S., Aaronson, S. A., Varmus, H. E. & Rubin, J. S. (1997) *Proc. Natl. Acad. Sci. USA* **94,** 6770–6775.
23. Leyns, L., Bouwmeester, T., Kim, S.-H., Piccolo, S. & DeRobertis, E. M. (1997) *Cell* **88,** 747–756.
24. Mayr, T., Deutsch, U., Kuhl, M., Drexler, H. C. A., Lottspeich, F., Deutzmann, R., Wedlich, D. & Risau, W. (1997) *Mech. Dev.* **63,** 109–125.
25. Melkonyan, H. S., Chang, W. C., Shapiro, J. P., Mahadevappa, M., Fitzpatrick, P. A., Kiefer, M. C., Tomei, L. D. & Umansky, S. R. (1997) *Proc. Natl. Acad. Sci. USA* **94,** 13636–13641.
26. Rattner, A., Hsieh, J.-C., Smallwood, P. M., Gilbert, D. J., Copeland, N. G., Jenkins, N. A. & Nathans, J. (1997) *Proc. Natl. Acad. Sci. USA* **94,** 2859–2863.
27. Salic, A., Kroll, K. L., Evans, L. M. & Kirschner, M. W. (1997) *Development (Cambridge, U.K.)* **124,** 4739–4748.
28. Wang, S. W., Krinks, M., Lin, K., Luyten, F. P. & Moos, M. (1997) *Cell* **88,** 757–766.
29. Katijewski, J., Mason, J. & Varmus, H. (1992) *Mol. Cell. Biol.* **12,** 784–790.
30. Bradley, R. S. & Brown, A. M. C. (1990) *EMBO J.* **9,** 1569–1575.
31. Papkoff, J. & Schryver, B. (1990) *Mol. Cell. Biol.* **10,** 2723–2730.
32. Burrus, L. W. & McMahon, A. P. (1995) *Exp. Cell Res.* **220,** 363–373.
33. van Leeuwen, F., Harryman Samos, C. & Nusse, R. (1994) *Nature (London)* **368,** 342–344.
34. Bradley, R. S. & Brown, A. M. C. (1995) *Mol. Cell. Biol.* **15,** 4616–4622.
35. Austin, T. W., Solar, G. P., Ziegler, F. C., Liem, L. & Mathews, W. (1997) *Blood* **89,** 3624–3635.
36. Christian, J. L. & Moon, R. T. (1993) *Genes Dev.* **7,** 13–28.
37. Cheng, H.-J., Nakamoto, M., Bergemann, A. D. & Flanagan, J. G. (1995) *Cell* **82,** 371–381.
38. Gorman, C. M., Gies, D. R. & McCray, G. (1990) *DNA Protein Eng. Tech.* **2,** 3–10.
39. Evan, G. I., Lewis, G. K., Ramsay, G. & Bishop, M. J. (1985) *Mol. Cell. Biol.* **5,** 3610–3616.
40. Caras, I., Weddell, G. N., Davitz, M. A., Nussenzweig, V. & Martin, D. W. (1987) *Science* **238,** 1280–1283.
41. Aruffo, A., Stamenkovic, I., Melnick, M., Underhill, C. B. & Seed, B. (1990) *Cell* **61,** 1303–1313.
42. Hoppler, S., Brown, J. D. & Moon, R. T. (1996) *Genes Dev.* **10,** 2805–2817.
43. Matsumura, M., Saito, Y., Jackson, M. R., Song, E. S. & Peterson, P. A. (1992) *J. Biol. Chem.* **267,** 23589–23595.
44. Hinck, L., Nelson, W. J. & Papkoff, J. (1994) *J. Cell Biol.* **124,** 729–741.
45. Klausner, R. D. & Sitia, R. (1990) *Cell* **62,** 611–614.
46. Creighton, T. E. (1984) *Proteins: Structures and Molecular Properties.* (Freeman, New York).
47. van den Heuvel, M., Harryman Samos, C., Klingensmith, J., Perrimon, N. & Nusse, R. (1993) *EMBO J.* **12,** 5293–5302.
48. Kadowaki, T., Wilder, E., Klingensmith, J., Zachary, K. & Perrimon, N. (1996) *Genes Dev.* **10,** 3116–3128.
49. Lin, K., Wang, S., Julius, M. A., Kitajewski, J., Moos, M. & Luyten, F. P. (1997) *Proc. Natl. Acad. Sci. USA* **94,** 11196–11200.
50. Reichsman, F., Smith, L. & Cumberledge, S. (1996) *J. Cell Biol.* **135,** 819–827.
51. Hsieh, J.-C., Kodjabachian, L., Rebbert, M., Rattner, A., Smallwood, P. M., Harryman Samos, C., Nusse, R., Dawid, I. & Nathans, J. (1999) *Nature (London)*, in press.
52. Binari, R. C., Staveley, B. E., Johnson, W. A., Godavarti, R., Sasisekharan, R. & Manoukian, A. S. (1997) *Development (Cambridge, U.K.)* **124,** 2623–2632.
53. Hacker, U., Lin, X. & Perrimon, N. (1997) *Development (Cambridge, U.K.)* **124,** 3565–3573.
54. Haerry, T. E., Heslip, T. R., Marsh, J. L. & O'Conner, M. B. (1997) *Development (Cambridge, U.K.)* **124,** 3529–3537.
55. Spivak-Kroizman, T., Lemmon, M. A., Dikic, I., Ladbury, J. E., Pinchasi, D., Huang, J., Jaye, M., Crumley, G., Schlessinger, J. & Lax, I. (1994) *Cell* **79,** 1015–1023.
56. Ornitz, D., Herr, A. B., Nilsson, M., Westman, J., Svahn, C.-M. & Waksman, G. (1995) *Science* **268,** 432–436.
57. Sherman, P. M., Sun, H., Macke, J. P., Williams, J., Smallwood, P. M. & Nathans, J. (1997) *Proc. Natl. Acad. Sci. USA* **94,** 11639–11644.